

# Excessive Costimulation Leads to Dysfunction of Adoptively Transferred T Cells

Dinali Wijewarnasuriya<sup>1,2</sup>, Christina Bebernitz<sup>1,2</sup>, Andrea V. Lopez<sup>2</sup>, Sarwish Rafiq<sup>3</sup>, and Renier J. Brentjens<sup>2,4,5</sup>

## ABSTRACT

Although clinical responses with CD19-targeting chimeric antigen receptor (CAR) T-cell treatment have been observed in patients with certain hematologic malignancies, high rates of disease relapse highlight the necessity to understand and improve mechanisms of CAR T-cell failure. Because T-cell dysfunction is thought to contribute to CAR T-cell treatment failure, understanding what mechanisms drive T cells into this dysfunctional state may aid optimal design of efficacious CAR T cells. Dysfunctional CAR T cells have been characterized as having upregulated inhibitory receptors and decreased cytolytic capabilities. Previous studies have identified a role for sustained CAR CD3 $\zeta$  signaling in CAR T-cell

dysfunction. Here, we demonstrate a mechanism that drives dysfunction in CAR T cells through excessive costimulation. Fully activated CD19-targeted CAR T cells were rendered dysfunctional upon stimulation with both endogenous CD28 stimulation and CAR-mediated CD28 costimulation. Costimulation-driven dysfunction of CAR T cells was demonstrated in a syngeneic immunocompetent mouse model, in which CAR T cells were activated with signals 1 (CD3 $\zeta$ ), 2 (CD28), and 3 (IL12). Thus, we show that CAR T-cell dysfunction can be driven through excessive CD28 and 4-1BB costimulation.

See related article by Drakes et al., p. 743

## Introduction

T-cell activation depends on T-cell receptor (TCR) engagement (signal 1), costimulation (signal 2), and inflammatory cytokines such as IL12 or type I IFNs (signal 3). T cells require signal 3 cytokine stimulation to develop optimal effector function, survival, and formation of memory T cells (1–3). T-cell dysfunction has been described as an alteration of the activation and differentiation process. Chronic antigen stimulation drives T cells into this dysfunctional state with reduced antiviral or antitumor effector function (1–4). These dysfunctional cells are characterized by overexpression and maintenance of multiple inhibitory receptors, impaired ability to produce effector cytokines, and loss of proliferative and cytotoxic capabilities (5–11).

T lymphocytes can be modified to have antitumor specificity through the incorporation of a chimeric antigen receptor (CAR) where the antigen recognition domain, such as a single chain variable fragment (scFv), is tethered to intracellular signaling domains (12–15). Once a CAR T cell recognizes and interacts with the target antigen, the CAR T cell becomes activated, proliferates, and lyses tumor targets (16, 17). Although CD19-directed CAR T-cell treatment of

hematologic malignancies has induced complete remission in a majority of patients, high rates of disease relapse indicate the necessity to enhance CAR T-cell functionality and persistence (18–23). CAR T-cell dysfunction is one mechanism of CAR T-cell treatment failure and has been described to be induced through the chronic phosphorylation of the CAR CD3 $\zeta$  domain (24–26). Upregulation of inhibitory receptors, such as PD-1, TIM-3, and LAG-3, has been observed on CAR T cells, suggesting that CAR T cells can be driven into a dysfunctional phenotype upon exposure to the tumor microenvironment (27, 28).

Although dysfunction driven by chronic TCR signaling has been previously demonstrated, the role of costimulation in T-cell dysfunction has not been established. Utilizing CAR T cells in a syngeneic mouse model, we demonstrate that fully activated CAR T cells receiving excessive costimulation become dysfunctional. Specifically, although a single costimulatory signal is necessary for optimal CAR T-cell function, excessive costimulatory signaling renders CAR T cells dysfunctional and unable to control tumor growth *in vivo*.

## Materials and Methods

### Cell lines

EL4 thymoma cells (Sigma-Aldrich, cat# 85023105-1VL) modified with truncated mouse CD19, MUC16<sup>ctd</sup>, or mCherry-luciferase were maintained in RPMI 1640 medium (Gibco) supplemented with 10% heat-inactivated FBS (Atlanta Biologicals), non-essential amino acids, sodium pyruvate, HEPES, L-glutamine, penicillin/streptomycin, and 2-mercaptoethanol (Invitrogen). EL4 thymoma cells were purchased in 2017 and were maintained in culture for approximately 2 to 3 months. Phoenix ecotropic packaging cells (ATCC CRL-3214) were maintained in DMEM supplemented with 10% FBS, L-glutamine, and penicillin/streptomycin. Phoenix ecotropic packaging cells were kindly provided by Michel Sadelain, Memorial Sloan Kettering Cancer Center, New York, NY, and were maintained in culture for approximately 2 to 3 months during experimental use. Cells were not authenticated in the past year. Cell lines were tested for mycoplasma using Lonza MycoAlert Detection Kit (cat# LT07-318). Murine T cells were maintained in RPMI,

<sup>1</sup>Weill Cornell Graduate School of Medical Sciences, New York, New York. <sup>2</sup>Department of Medicine, Memorial Sloan Kettering Cancer Center, New York, New York. <sup>3</sup>Department of Hematology and Medical Oncology, Winship Cancer Institute of Emory University School of Medicine, Atlanta, Georgia. <sup>4</sup>Cellular Therapeutics Center, Memorial Sloan Kettering Cancer Center, New York, New York. <sup>5</sup>Department of Pharmacology, Weill Cornell Graduate School of Medical Sciences, New York, New York.

**Note:** Supplementary data for this article are available at Cancer Immunology Research Online (<http://cancerimmunolres.aacrjournals.org/>).

**Corresponding Author:** Renier J. Brentjens, Memorial Sloan Kettering Cancer Center, Box#242, 1275 York Avenue, New York, NY 10065. Phone: 212-639-7053; Fax: 212-772-8441; E-mail: [brentjer@mskcc.org](mailto:brentjer@mskcc.org)

Cancer Immunol Res 2020;8:732–42

doi: 10.1158/2326-6066.CIR-19-0908

©2020 American Association for Cancer Research.

supplemented as described above, with 100 IU/mL rhIL2 (Novartis Pharmaceuticals).

### ***In vivo* models**

C57BL/6 (000664), CD28<sup>-/-</sup> (B6.129S2-CD28tm1Mak/J; 002666), and CD80/86<sup>-/-</sup> (B6.129S4-CD80<sup>tm1Shr</sup>CD86<sup>tm2Shr</sup>/J; 003610) mice were obtained from The Jackson laboratory. Mice were inoculated i.v. with  $1 \times 10^6$  EL4mCD19 or EL4(MUC16<sup>ecto</sup>) tumor cells and then treated with  $3 \times 10^6$  CAR T cells i.v. the following day. *Ex vivo* studies were conducted on mice treated with  $9 \times 10^6$  CAR T cells, containing a vexGFP tag, i.v. 5 or 10 days after treatment. CAR T cells were isolated from the bone marrow or spleen through fluorescence-activated cell sorting (FACS) detection of vexGFP tag. Isolated CAR T cells were then cocultured at a 1:1 ratio with tumor cells expressing luciferase. Cytotoxicity assay was then performed as described below. Mice preconditioned with cyclophosphamide were injected with 250 mg/kg -3 days before inoculation with tumor cells. Mice were not pretreated with cyclophosphamide unless otherwise noted. All animal studies were performed according to Memorial Sloan Kettering Cancer Center Institutional Animal Care and Use Committee-approved protocol (00-05-065).

### **Construct generation**

SFG-19z vector (13, 29) was modified by exchange of the anti-human CD19 scFv with a murine CD19 targeting scFv (30, 31). Mouse CD28 transmembrane domain was fused to mouse CD3 $\zeta$  chain and scFv. Murine IL12 (mIL12f) fusion gene (29) was modified with CD8 (32) leader peptide, internal ribosome entry site, and with serine-glycine repeats between p35 and p40 chains. CAR T-cell sequences are in Supplementary Fig. S1. mIL12f was kindly provided by Alan Houghton and Jedd Wolchok, Memorial Sloan Kettering Cancer Center, New York, NY (33).

### **Transduction of mouse T cells**

Murine T cells were isolated from the spleens of euthanized mice and enriched with nylon wool fiber columns (Polysciences; ref. 32). T cells were subsequently activated with CD3/CD28 Dynabeads (Invitrogen; ratio 1:2). Retroviral transduction into murine T cells was performed as previously described (32). Briefly, CAR transduction was achieved by spinoculating (3,200 rpm for 60 minutes) murine T cells on retronectin-coated (Takara Clontech) plates with retroviral supernatant from Phoenix packaging cells.

### **Cytotoxicity assays**

Cytolytic capacity of murine CAR T cells was assessed through luciferase killing assay (34). CAR T cells were cocultured with target cells, EL4mCD19 tumor cells that expressed mCherry firefly-luciferase (ffLuc), at various effector-to-target ratios in a total volume of 200  $\mu$ L of cell media. Target cells alone were plated at the same cell density to determine the maximal luciferase expression as a reference (“max signal”). Four or 24 hours later, 75 ng of D-luciferin (Gold Biotechnology) dissolved in 5  $\mu$ L of PBS was added to each well. Bioluminescence was assessed, by Tecan Spark microplate reader (TECAN), 4 or 24 hours after coculture. *Ex vivo* cytotoxicity assays were conducted with CAR T cells isolated from bone marrow with FACS. CAR T cells were isolated by detection of violet-excitatable GFP tag fused to the CAR with FACS Aria (BD Biosciences) and then cocultured with EL4mCD19 tumor targets (mCherry-ffLuc<sup>+</sup>) for 24 hours. Percent lysis was determined as  $[1 - (\text{“sample signal”}/\text{“max signal”})] \times 100$ .

### **Flow cytometry analysis**

Note that 10-color Gallios B43618 (Beckman Coulter) and 14-color Attune NxT (Thermo Fisher Scientific) were used to acquire data. Analysis was performed with FlowJo software. Cells were counted with 123count eBeads (Thermo Fisher). Expression of CAR was detected by myc tag (9E10, Alexa Fluor 647, Thermo Fisher) or violet-excitatable GFP tag. DAPI (0.5 mg/mL, Sigma-Aldrich) or a LIVE/DEAD fixable yellow fluorescent dye (Thermo Fisher) was used to exclude dead cells in all experiments. Sorting of splenocytes after tissue processing was done using a BD FACSAria under sterile conditions. Antibodies to the following mouse proteins were used for flow cytometry: CD3e (145-2C11, eBioscience, cat# 11-0031-85), CD3 (17A2, BioLegend, cat# 100233), CD4 (GK1.5, eBioscience, cat# 48-0041-80), CD4 (RM4-5, eBioscience, cat# 69-0042-80), CD8 $\alpha$  (53-6.7, eBioscience, cat# 48-0041-80), CD19 (eBio1D3, eBioscience, cat# 48-0193-82), CD25 (PC61.5, eBioscience, cat# 25-0251-81), CD45 (30-F11, BioLegend, cat# 103106), CD80 (16-10A1, eBioscience, cat# 46-0801), CD86 (GL1, eBioscience, cat# 25-0862), CD223 LAG-3 (C9B7W, eBioscience, cat# 12-5956-80), CD279 PD-1 (J43, eBioscience, cat# 48-9985-82), and TIM3 (8B.2C12, eBioscience, cat# 48-5871-80).

### **Cytokine analyses**

A Luminex IS100 machine was used to detect cytokines with the MILLIPLEX MAP mouse cytokine/chemokine, premixed, 10 Plex kit. Murine T cells were cocultured with tumor targets at a 1:1 ratio for 24 hours in a 96-well round-bottom plate in 200  $\mu$ L of media. The supernatant fluid was collected and analyzed for cytokines on a Luminex IS100 instrument. Luminex FlexMap3D system and Luminex Xponent 4.2 (Millipore Corporation) were used to detect the cytokines.

### **Serum T-cell analysis**

Whole blood was collected from mice, and serum was prepared by allowing the blood to clot with centrifugation at 14,000 rpm for 30 minutes at 4°C. Red blood cell lysis was achieved with an ammonium-chloride-potassium Lysing Buffer (Lonza). T cells were washed with PBS and used for subsequent flow cytometry analysis.

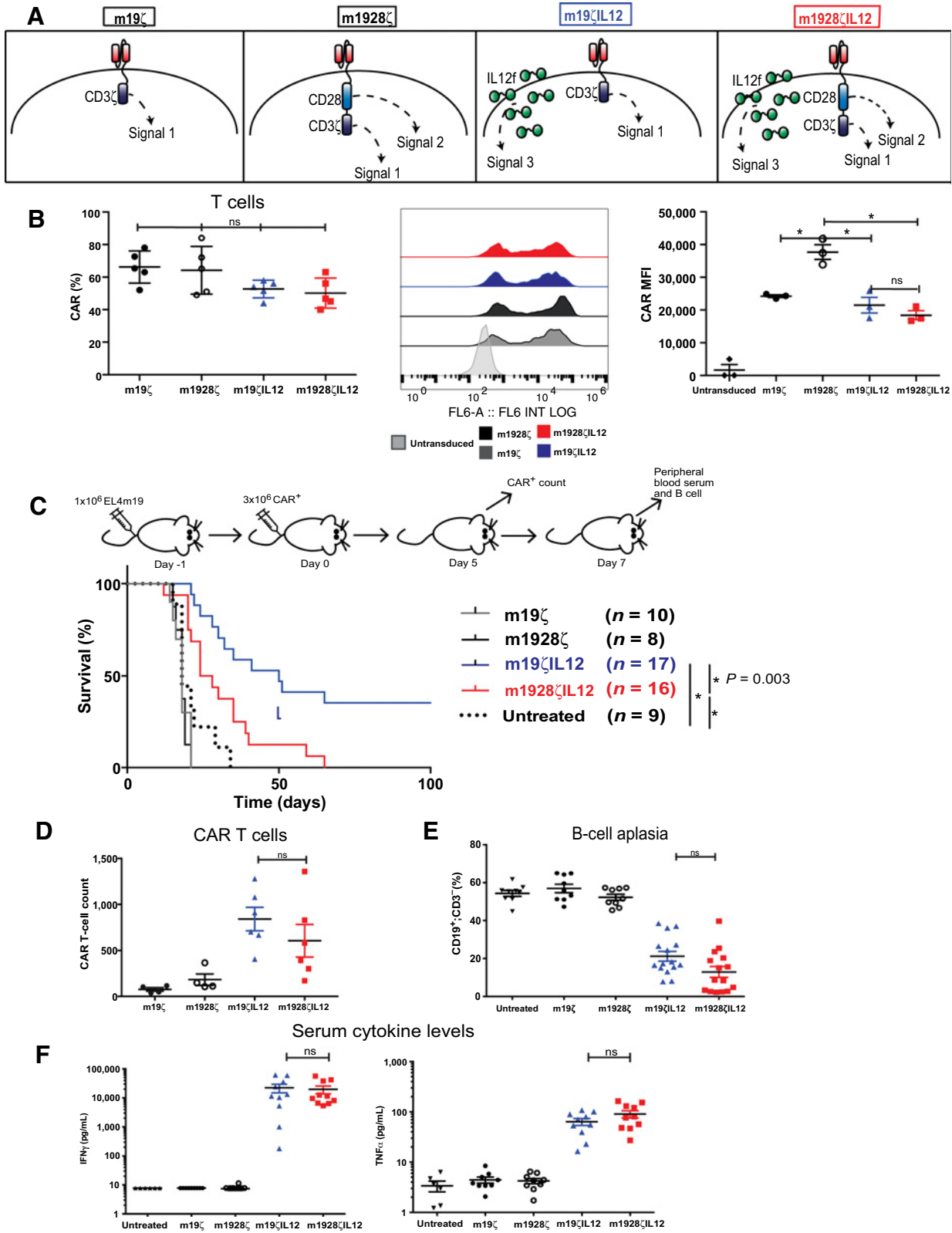
### **Quantification and statistical analysis**

All statistical analyses were performed using GraphPad Prism software (GraphPad). Data points represent biological replicates and are shown as the mean  $\pm$  SEM as indicated in the figure legends. Statistical significance was determined using an unpaired two-tailed Student *t* test, one-way ANOVA, or two-way ANOVA as indicated in the figure legends. The log-rank (Mantel-Cox) test was used to determine statistical significance for overall survival in mouse survival experiments.

## **Results**

### **CAR T cells engineered with CD28 and IL12 become dysfunctional *in vivo***

To investigate the optimal T-cell activation signals for CAR T-cell efficacy, we generated CAR constructs targeting mouse CD19 (m19) to conduct this study in a fully syngeneic mouse model. First-generation m19 $\zeta$  CAR T cells are composed of a CD3 $\zeta$  signal transduction domain (signal 1), whereas second-generation m1928 $\zeta$  CAR T cells include the additional CD28 costimulation signaling domain (signal 2; Supplementary Fig. S1). m19 $\zeta$  CAR and m1928 $\zeta$  CAR constructs were further modified to secrete murine IL12  $\alpha$  and  $\beta$  subunit fusion protein (IL12f) providing signal 3 to the T cell (m19 $\zeta$ IL12 CAR and



m1928 $\zeta$ IL12 CAR), which is necessary for full T-cell activation (Fig. 1A; Supplementary Fig. S1; refs. 35–37). Gene transfer efficiency of CAR constructs into mouse T cells was comparable between all constructs (Fig. 1B). IL12 was secreted only from IL12-secreting CAR T cells (Supplementary Fig. S2A).

To determine CAR T-cell effector function *in vivo*, C57BL/6 mice were inoculated with a systemic EL4 thymoma tumor modified to express a truncated mouse CD19 (EL4mCD19). m19 $\zeta$  and m1928 $\zeta$  CAR T cells are capable of eradicating tumor in mice pretreated with cyclophosphamide (Supplementary Fig. S2B), indicating that m19 $\zeta$  and m1928 $\zeta$  CAR T cells were functional. Consistent with previously reported findings (29), m19 $\zeta$  and m1928 $\zeta$  CAR T-cell-treated mice fail to eradicate tumor without cyclophosphamide preconditioning (Fig. 1C). m19 $\zeta$ IL12 CAR T-cell-treated mice show enhanced survival compared with all treatment groups indicating improved efficacy with the addition of IL12 to m19 $\zeta$  CAR T cells (Fig. 1C). Addition of IL12 to the m1928 $\zeta$  CAR construct (m1928 $\zeta$ IL12-treated mice) resulted in decreased survival when compared with m19 $\zeta$ IL12 CAR T-cell-treated mice (Fig. 1C).

Before injection, m19 $\zeta$ IL12 and m1928 $\zeta$ IL12 CAR T cells expressed equivalent amounts of activation marker CD25 and lysed tumor targets with equal effectiveness *in vitro* (Supplementary Fig. S2C and S2D). CAR T-cell expansion *in vivo* was not significantly different between m19 $\zeta$ IL12- and m1928 $\zeta$ IL12-treated mice (Fig. 1D). As CD19-targeted CAR T cells lyse CD19<sup>+</sup> B cells in addition to tumor cells, B-cell aplasia can be utilized as a surrogate marker for CAR T-cell functionality and persistence. Both IL12-secreting CAR T cells were functional and capable of inducing relative B-cell aplasia (Fig. 1E). Peripheral blood analysis demonstrated increased IFN $\gamma$  and TNF $\alpha$  in both cohorts of mice treated with IL12-secreting CAR T cells (Fig. 1F). Systemic IL12 was not detected in the peripheral blood of mice treated with IL12-secreting CAR T cells (Supplementary Fig. S2E). These results show that differences in trafficking, proliferation, and cytokine secretion between the types of IL12-secreting CAR T cells (m19 $\zeta$ IL12 and m1928 $\zeta$ IL12) did not account for differences in the enhancement of survival of tumor-bearing mice.

We next investigated the immunophenotype of CAR T cells *in vivo* (Fig. 2A; Supplementary Fig. S3A and S3B). Dysfunctional T cells can be characterized by the overexpression and maintenance of multiple inhibitory receptors such as PD-1, TIM-3, or LAG-3 (9–11, 38). CAR T cells isolated from mice treated with m1928 $\zeta$ IL12 CAR T cells expressed increased amounts of inhibitory receptors TIM-3, LAG-3, and PD-1 compared with those from mice treated with m19 $\zeta$ IL12 CAR T cells, indicating a dysfunctional phenotype *in vivo* (Fig. 2B; Supplementary Fig. S4A and S4B). To further assess functionality, CAR T cells were isolated by FACS and cocultured with EL4mCD19 tumor targets *ex vivo*. Although m19 $\zeta$ IL12 CAR T cells were still capable of

lysing tumor targets, m1928 $\zeta$ IL12 CAR T cells failed to kill tumor targets (Fig. 2C). Taken together, these data indicate that m1928 $\zeta$ IL12 CAR T cells become dysfunctional *in vivo*, whereas m19 $\zeta$ IL12 CAR T cells retain cytolytic function.

We next looked at the CD8<sup>+</sup> to CD4<sup>+</sup> ratio of the CAR T cells to determine if the difference in inhibitory receptor expression and cytolytic function was skewed due to differences in the CD8<sup>+</sup> to CD4<sup>+</sup> ratio. Although the CD8<sup>+</sup> to CD4<sup>+</sup> ratio of the CAR T cells was similar at day 0, before injection into tumor-bearing mice (Supplementary Fig. S5A), m19 $\zeta$ IL12 CAR T cells had a higher CD8<sup>+</sup> to CD4<sup>+</sup> ratio compared with m1928 $\zeta$ IL12 CAR T cells *in vivo* (Fig. 2D; Supplementary Fig. S5B). We next looked at expression of inhibitory receptors TIM-3, LAG-3, and PD-1 on CD8<sup>+</sup> CAR T cells and observed that m1928 $\zeta$ IL12 CAR T cells expressed more inhibitory receptors compared with CD8<sup>+</sup> m19 $\zeta$ IL12 CAR T cells (Fig. 2E; Supplementary Fig. S5C and S5D). When isolated CD8<sup>+</sup> CAR T cells were cocultured with EL4mCD19 tumor targets *ex vivo*, CD8<sup>+</sup> m1928 $\zeta$ IL12 CAR T cells failed to kill tumor targets, whereas m19 $\zeta$ IL12 CAR T cells remained capable of lysing tumor (Fig. 2F). These data suggest that the dysfunctional phenotype of m1928 $\zeta$ IL12 CAR T cells is not due to the difference in CD8<sup>+</sup> to CD4<sup>+</sup> ratios.

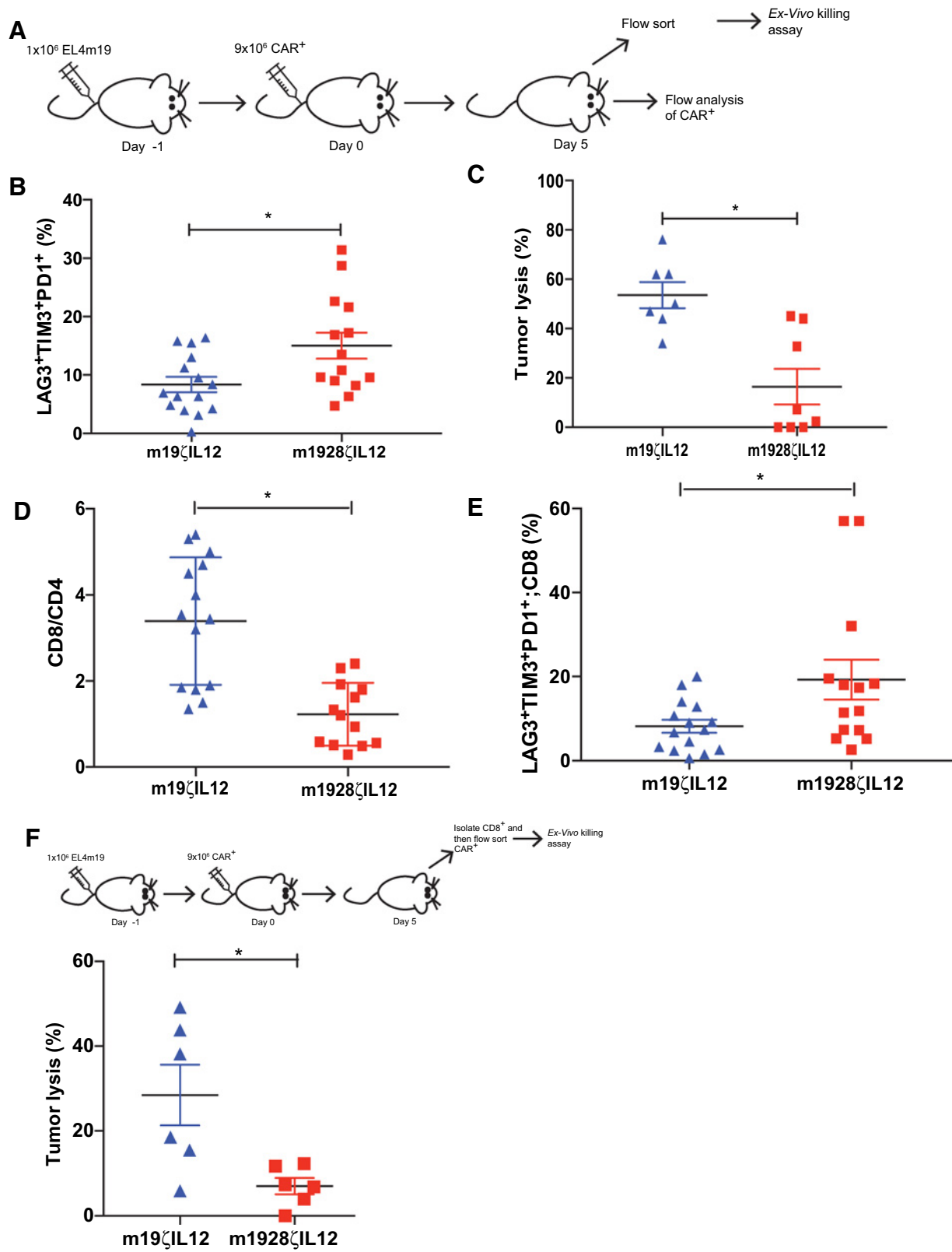
### Excessive costimulation drives IL12-secreting CAR T cells into T-cell dysfunction

Because CD19-targeted CAR T cells also recognize and lyse CD19-expressing endogenous B cells, we hypothesized that m1928 $\zeta$ IL12 CAR T cells become dysfunctional due to overstimulation. To investigate how B cells could be overstimulating CD19-targeted CAR T cells, we characterized the endogenous B cells and observed that B cells in EL4 tumor-bearing mice upregulate CD80, the CD28 ligand (Supplementary Fig. S6A). EL4 tumor cells secrete IL4, which induces CD80 upregulation on B cells (Supplementary Fig. S6B; ref. 39). This observation suggests that endogenous CD28 stimulation may occur when CD19-targeted CAR T cells interact with and lyse endogenous B cells.

In conventional CAR constructs, signal 2 is coupled with signal 1 (i.e., CD28 to CD3 $\zeta$ ). We hypothesized that overstimulation and eventual dysfunction of CAR T cells could be driven through the endogenous CD28 receptor. To test the role of excessive CD28 stimulation in CAR T-cell dysfunction, we compared CAR T cells generated from wild-type versus CD28<sup>-/-</sup> murine T cells (Supplementary Fig. S6C). CD28<sup>-/-</sup> CAR T cells were as effective at lysing tumor targets as were wild-type T cells (Supplementary Fig. S6D), indicating that loss of the endogenous CD28 receptor did not affect T-cell cytotoxicity. In wild-type m19 $\zeta$ IL12 CAR T cells, the CAR provides signal 1 and 3, whereas signal 2 can be provided through the endogenous CD28 receptor. m19 $\zeta$ IL12 CD28<sup>-/-</sup> T cells receive signals 1 and

### Figure 1.

CAR T cells engineered with CD28 and IL12 fail to sustain antitumor efficacy. **A**, Schematic representation of CAR T cells. **B**, Flow cytometry data demonstrating CAR expression in mouse T cells in terms of percentage, representative flow cytometry plot, and mean fluorescence intensity (MFI). Data shown are the mean  $\pm$  SEM with a total *n* of 5 per group of three independent experiments. Significance was determined through one-way ANOVA. MFI CAR expression: \*, *P* = 0.0022, m1928 $\zeta$  compared with m19 $\zeta$ ; \*, *P* = 0.0005, m1928 $\zeta$  compared with m19 $\zeta$ IL12; \*, *P* = 0.0001, m1928 $\zeta$  compared with m1928 $\zeta$ IL12. **C**, EL4mCD19 tumor-bearing C57BL/6 mice, not pretreated with cyclophosphamide, treated intravenously with CAR T cells. Significance determined through log-rank Mantel-Cox test, with 95% confidence interval. Data shown are from three independent experiments (*n* of 9–17 per group). m19 $\zeta$ IL12 compared with untreated \*, *P* < 0.001; m1928 $\zeta$ IL12 compared with untreated \*, *P* = 0.0129; m19 $\zeta$ IL12 compared with m1928 $\zeta$ IL12 \*, *P* = 0.0033. **D**, CAR T-cell counts normalized to total cell count obtained from bone marrow day 5 after treatment. CAR T cells were identified by vex-GFP tag through flow cytometry. Significance determined through one-way ANOVA. Data shown are the mean  $\pm$  SEM of three independent experiments (*n* = 4–6 mice per group). **E**, Peripheral blood obtained on day 7 after treatment was assessed for B-cell aplasia by detecting CD19<sup>+</sup>CD3<sup>-</sup> cells through flow cytometry. Significance determined through one-way ANOVA. Data shown are the mean  $\pm$  SEM of three independent experiments (*n* = 9–15 mice per group). **F**, Serum was assessed for IFN $\gamma$  and TNF $\alpha$  through Luminex on day 7 after CAR T-cell treatment. Significance determined through one-way ANOVA. Data shown are the mean  $\pm$  SEM of three independent experiments (*n* = 6–10 mice per group). ns, not significant.





3 through the CAR construct (Fig. 3A). m1928 $\zeta$ IL12 CD28<sup>-/-</sup> T cells receive signals 1, 2, and 3 through the CAR construct. Wild-type m1928 $\zeta$ IL12 T cells receive an additional signal 2 through the endogenous CD28 receptor (Fig. 3A). We observed that CD28<sup>-/-</sup> m1928 $\zeta$ IL12 CAR T cells, in contrast to wild-type m1928 $\zeta$ IL12 CAR T cells, prolonged survival of EL4mCD19 tumor-bearing mice (Fig. 3B). This result demonstrates that, in the absence of the endogenous CD28 receptor m1928 $\zeta$ IL12, CAR T cells can control tumor growth and suggests that additional CD28 signaling, through the second-generation CAR, is detrimental to CAR T-cell function. Furthermore, treatment of mice with CD28<sup>-/-</sup> m19 $\zeta$ IL12 CAR T cells, in contrast to treatment with wild-type m19 $\zeta$ IL12 CAR T cells, failed to promote survival, indicating the necessity of signal 2 for proper T-cell function (Fig. 3B). CD28<sup>-/-</sup> m1928 $\zeta$ IL12 CAR T cells displayed significantly enhanced lysis of CD19<sup>+</sup> tumor targets *ex vivo* compared with wild-type m1928 $\zeta$ IL12 CAR T cells (Fig. 3C), indicating that CD28<sup>-/-</sup> m1928 $\zeta$ IL12 CAR T cells, lacking costimulation through the endogenous CD28 receptor, retained T-cell function *in vivo*.

To confirm CAR T-cell dysfunction was driven through endogenous CD28 and CD80 interaction, we treated CD80/86<sup>-/-</sup> C57BL/6 mice with wild-type CAR T cells. In this model, all cells, including B cells, are CD80/86<sup>-/-</sup> and therefore unable to stimulate the CD28 receptor on CAR T cells. EL4 tumor cells are negative for CD80/86. CD80/86<sup>-/-</sup> tumor-bearing mice treated with wild-type m1928 $\zeta$ IL12 CAR T cells displayed prolonged survival similarly to wild-type tumor-bearing mice treated with wild-type m19 $\zeta$ IL12 CAR T cells (Fig. 3D). When CD80/86 is not present, m1928 $\zeta$ IL12 CAR T cells are able to control tumor. These data suggest IL12-secreting CAR T cells require CD28 costimulation but also that receiving CD28 costimulation through both the endogenous receptor and CAR construct leads to T-cell dysfunction. In other words, either too much or too little CD28 stimulation is detrimental for CAR T-cell function.

#### CAR T cells retain effector function when additional CD28 costimulation is not received

To determine if B-cell stimulation plays a role in CD19-targeted CAR T-cell dysfunction, we engineered a model in which CAR T cells do not target endogenous B cells. Mice inoculated with an EL4 tumor cell line expressing MUC16<sup>ecto</sup> were treated with CAR T cells composed with the 4h11 scFv targeting MUC16<sup>ecto</sup> (40, 41), the retained subunit of the cancer antigen 125 (CA125) commonly overexpressed on ovarian cancer. As expected, B-cell aplasia was not induced upon CAR T-cell treatment because 4h11-CAR T cells do not target CD19<sup>+</sup> B cells (Fig. 4A). In this model, 4h1128 $\zeta$ IL12 CAR T cells eradicated tumor and prolonged mouse survival (Fig. 4B). Increased IFN $\gamma$  and TNF $\alpha$  expression was detected in mice treated with 4h1128 $\zeta$ IL12 CAR T cells, indicating CAR T-cell

activation (Fig. 4C). In contrast to m1928 $\zeta$ IL12 CAR T cells, isolated 4h1128 $\zeta$ IL12 CAR T cells retained functionality and were capable of killing tumor targets *ex vivo* (Fig. 4D). These data, as predicted, demonstrate that when second-generation IL12-secreting CAR T cells are not targeted against endogenous antigens providing additional costimulation through the native CD28 receptor, CAR T cells do not become dysfunctional.

#### Excessive CD28 and 4-1BB costimulation can drive T-cell dysfunction

To investigate if excessive costimulation-driven T-cell dysfunction in IL12-secreting CAR T cells was specific to CD28 costimulation, we generated IL12-secreting CAR constructs with an alternate costimulation domain (m19BB $\zeta$ IL12; Supplementary Fig. S1). EL4mCD19 tumor-bearing mice treated with m19BB $\zeta$ IL12 CAR T cells succumbed to tumor-related death similar to m1928 $\zeta$ IL12 CAR T-cell-treated mice (Fig. 5A). CD8<sup>+</sup> m19BB $\zeta$ IL12 CAR T cells isolated day 5 after injection were not able to lyse EL4mCD19 tumor *ex vivo* (Fig. 5B), indicating a dysfunctional phenotype. These results suggest that costimulation-driven T-cell dysfunction is not limited to CD28 stimulation and that culminative costimulation through multiple pathways, such as 4-1BB plus CD28, can also drive T-cell dysfunction.

## Discussion

Because chronic TCR stimulation can induce T-cell dysfunction, constitutive CAR signaling is being investigated as a mechanism of rendering CAR T cells dysfunctional. Methods of restricting chronic CD3 $\zeta$  CAR signaling, such as mutating immunoreceptor tyrosine-based activation motif (ITAM) domains or inducing CAR protein degradation, have been shown to be effective in increasing antitumor efficacy of CAR T cells (25, 31). Because our data indicate that chronic CD28 signaling drives CAR T-cell dysfunction, attenuation of CD28 signaling may lead to CAR T cells with increased antitumor efficacy (42). Second-generation fibroblast activation protein (FAP)-specific CAR T cells demonstrated increased antitumor efficacy when the Lck-binding domain of CD28 was deleted (42). CD19-specific CAR T cells mutated at the YMN domain secreted less IFN $\gamma$ , drove less TCR signaling determined through Nur77 expression, and showed increased CAR T-cell persistence *in vivo* (43). Thus, attenuation of CAR CD28 signaling can prevent CAR T-cell dysfunction and improve CAR T-cell functionality.

We further show that costimulation-driven CAR T-cell dysfunction can be induced through 4-1BB costimulation as well as CD28 costimulation. Although differences in persistence and dysfunction have been shown between CAR T cells containing either the 4-1BB or CD28 costimulation domain, both CAR constructs activate similar phosphoprotein signaling pathways, albeit with differing signaling strength and kinetics (44). Here, we show that when the endogenous CD28 is

#### Figure 2.

CAR T cells engineered with CD28 and IL12 become dysfunctional *in vivo*. **A**, Schematic diagram of experimental setup to analyze CAR T cells. C57BL/6 mice were inoculated with EL4mCD19 tumor day -1 and treated with CAR T cells intravenously day 0. CAR T cells were analyzed or isolated by FACS day 5 or day 10 from the bone marrow and spleen. **B**, CAR T cells, day 5 after infusion, were characterized by flow cytometry. Data shown are the mean  $\pm$  SEM of three independent experiments. Significance of \*,  $P = 0.0146$  was determined by unpaired  $t$  test ( $n = 14-15$  per group). **C**, CAR T cells were isolated by FACS from the bone marrow, cocultured with EL4mCD19 tumor targets, and then assessed for cytotoxicity 24 hours later, using a luciferase killing assay. Data shown are the mean  $\pm$  SEM of three independent experiments. Significance of \*,  $P = 0.0014$  was determined by unpaired  $t$  test ( $n = 7-8$  per group). **D**, CAR T cells, day 5 after infusion, were characterized by flow cytometry. Data shown are the mean  $\pm$  SEM of three independent experiments. Significance of \*,  $P < 0.0001$  was determined by unpaired  $t$  test ( $n = 13-14$  per group). **E**, CD8<sup>+</sup> CAR T cells, day 5 after infusion, were characterized by flow cytometry. Data shown are the mean  $\pm$  SEM of three independent experiments. Significance of \*,  $P = 0.0301$  was determined by unpaired  $t$  test ( $n = 14-15$  per group). **F**, CAR T cells were isolated by FACS from the bone marrow, selected for CD8<sup>+</sup> T cells, cocultured with EL4mCD19 tumor targets, and then assessed for cytotoxicity 24 hours later, using a luciferase killing assay. Data shown are mean  $\pm$  SEM of three independent experiments. Significance of \*,  $P = 0.0155$  was determined by one-way ANOVA ( $n = 6$  per group).

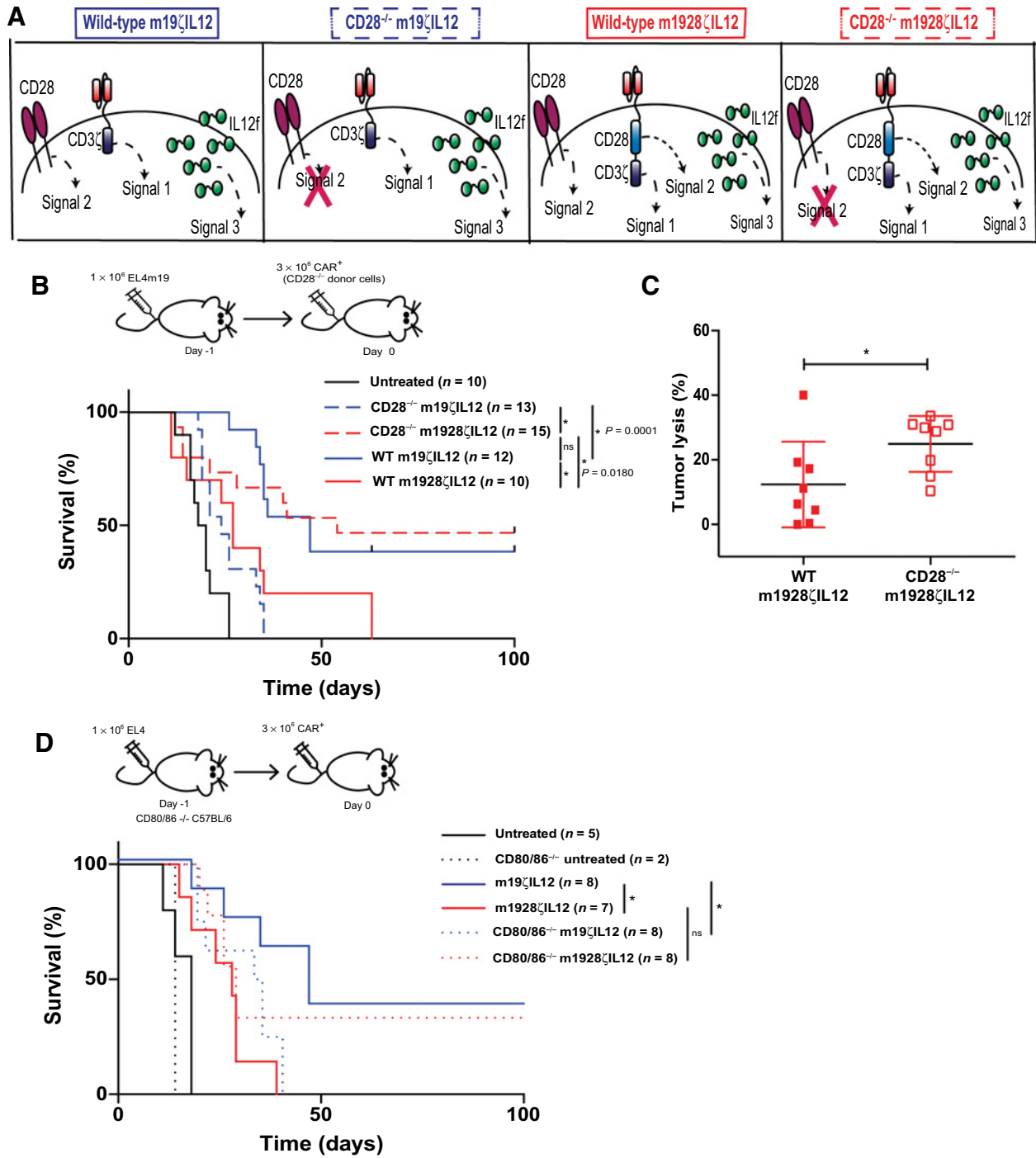


**Figure 3.**

Excessive costimulation drives IL12-secreting CAR T cells into dysfunction. **A**, Schematic diagram of experimental setup. When endogenous CD28 is knocked out, m19 $\zeta$ IL12 CAR T cells can receive only signals 1 and 3, whereas m1928 $\zeta$ IL12 CAR T cells receive signals 1, 2, and 3. **B**, EL4mCD19 tumor-bearing C57BL/6 mice, not pretreated with cyclophosphamide, treated with CD28<sup>-/-</sup> or wild-type CAR T cells. Data were obtained from three independent experiments, and significance was determined through log-rank Mantel-Cox test, with 95% confidence interval ( $n = 10$ – $15$  mice per group). CD28<sup>-/-</sup> m19 $\zeta$ IL12 compared with m19 $\zeta$ IL12 \*,  $P < 0.0001$ ; CD28<sup>-/-</sup> m1928 $\zeta$ IL12 compared with m1928 $\zeta$ IL12 \*,  $P = 0.0180$ ; CD28<sup>-/-</sup> m19 $\zeta$ IL12 compared with CD28<sup>-/-</sup> m1928 $\zeta$ IL12 \*,  $P = 0.0019$ ; m19 $\zeta$ IL12 compared with m1928 $\zeta$ IL12 \*,  $P = 0.0100$ ; and CD28<sup>-/-</sup> m1928 $\zeta$ IL12 compared with m19 $\zeta$ IL12 “ns.” **C**, Five days after treatment, CAR T cells were flow sorted from the bone marrow, cocultured with EL4mCD19 tumor targets, and then assessed for cytotoxicity 24 hours later, using a luciferase killing assay. Data shown are the mean  $\pm$  SEM of two independent experiments. Significance of \*,  $P = 0.0417$  was determined by unpaired  $t$  test ( $n = 8$  per group). **D**, CD80/86<sup>-/-</sup> C57BL/6 mice were injected intravenously with EL4mCD19 tumor and treated with CAR T cells 1 day later. Data were obtained from two independent experiments, and significance was determined through log-rank Mantel-Cox test, with 95% confidence interval ( $n = 2$ – $8$  mice per group). ns, not significant.

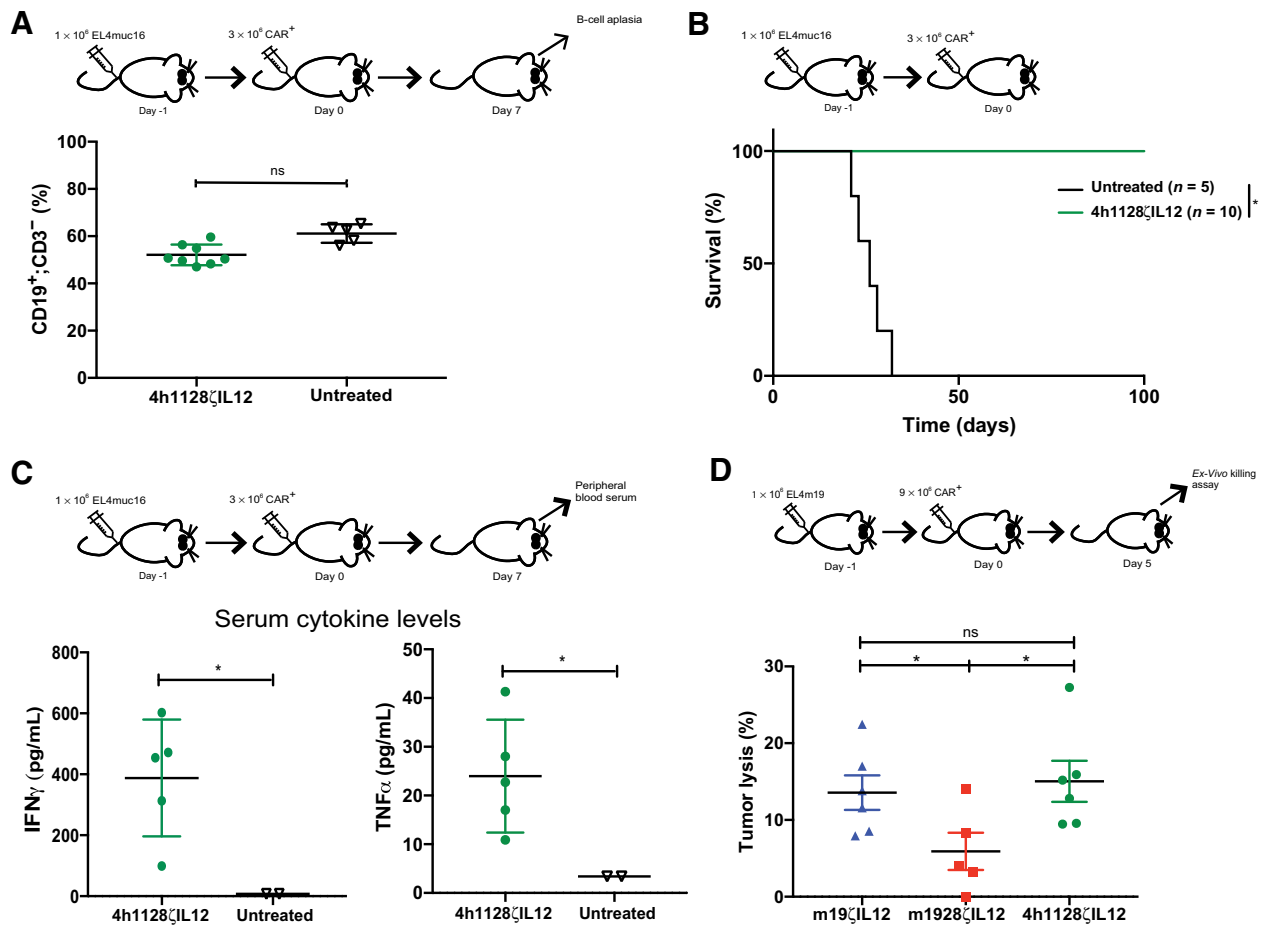


**Figure 4.**

CAR T cells retain effector function when additional CD28 costimulation is not received. **A**, Peripheral blood was assessed for B-cell aplasia by detecting CD19<sup>+</sup>CD3<sup>-</sup> cells through flow cytometry. Relative B-cell aplasia was not observed as CAR T cells were targeted toward MUC16<sup>ecto</sup> (ns by unpaired *t* test). Data shown are mean ± SEM of three independent experiments (*n* = 5–8 per group). **B**, C57BL/6 mice were injected intravenously with EL4(MUC16<sup>ecto</sup>) tumor cells and then treated with CAR T cells 1 day later. The percentage of survival is indicated. Data were obtained from two independent experiments, and the significance of \*, *P* ≤ 0.0001 was determined through log-rank Mantel-Cox test, with 95% confidence interval (*n* = 5–10 mice per group). **C**, C57BL/6 mice were injected intravenously with EL4 (MUC16<sup>ecto</sup>) tumor cells and treated with CAR T cells 1 day later. Seven days later, IFN $\gamma$  and TNF $\alpha$  cytokine concentrations in the peripheral blood were measured. Significance determined through one-way ANOVA (*n* = 2–5 mice per group). Data shown are the mean ± SEM of two independent experiments. **D**, CAR T cells were isolated by FACS from the bone marrow, cocultured with EL4 (MUC16<sup>ecto</sup>; luciferase) tumor targets, and then assessed for cytotoxicity 24 hours later, using a luciferase killing assay. Data shown are mean ± SEM of two independent experiments. Significance of \*, *P* = 0.0351 was determined by unpaired *t* test (*n* = 5–6 per group). ns, not significant.

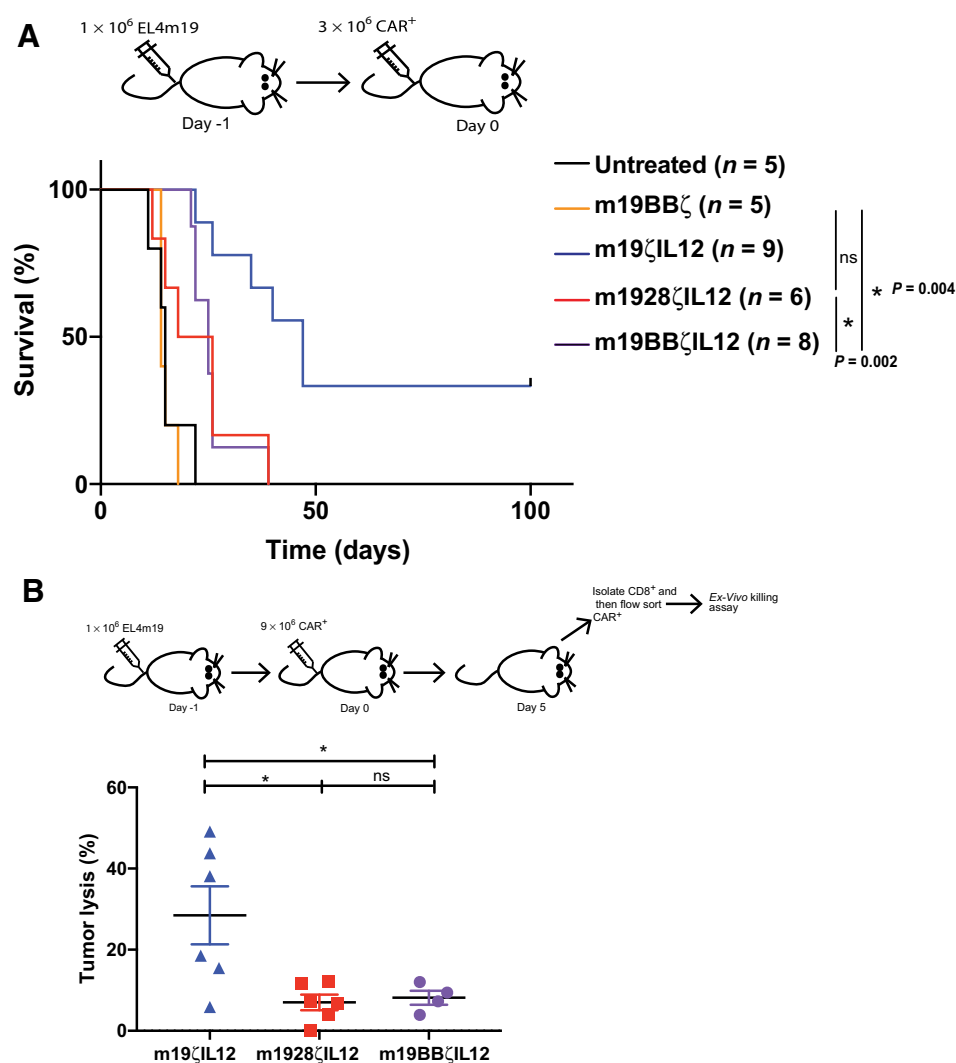
stimulated in the context of IL12, CAR T-cell dysfunction can be driven through either the CAR 4-1BB or CAR CD28 domains. Thus, costimulation-driven dysfunction is not specific to CD28 costimulation.

CARs have increased affinity toward target antigens due to the antibody-based scFv when compared with the binding of the native TCR to a peptide–MHC complex. Comparison of a native  $\alpha\beta$  TCR with a TCR-like antibody specific to the same target demonstrated that CAR T cells based on a native low-affinity  $\alpha\beta$  TCR maintained antitumor cytotoxic function, whereas CAR T cells based on the high-affinity TCR-like antibody exhibited decreased cytotoxic function (45). It is possible the CAR CD28 signaling kinetics result in excess CD28 signal transduction that when combined with the native endogenous CD28 signaling pushes the m1928ζIL12 CAR T cells into a dysfunctional state. Future experiments need to be conducted to investigate the signaling kinetics of the endogenous CD28 receptor compared with the CAR-mediated CD28 signaling domain.

Previous work has demonstrated that in an EL4 tumor-bearing syngeneic mouse model, CAR secretion of IL12 was necessary for antitumor efficacy when mice were not preconditioned with cyclophosphamide (29). CAR T-cell dysfunction was not observed when a CD19-specific second-generation IL18-secreting CAR T cell was used to treat EL4 tumor-bearing immunocompetent mice (46). IL18 has not been known to provide activation signal 3 to T cells. This result implies that excessive costimulation drives CAR T-cell dysfunction only when CAR T cells are fully activated with all three T-cell activation signals, including IL12 (signal 3) cytokine stimulation. Further experiments need to be conducted to determine the role of IL12 in excessive costimulation-driven dysfunction of CAR T cells.

Further analysis of this work in human T cells would be necessary to determine if excessive CD28 costimulation drives dysfunction of human CAR T cells. Although we were able to demonstrate costimulation-driven dysfunction in a syngeneic mouse model, further



**Figure 5.**

Excessive CD28 and 4-1BB costimulation can drive T-cell dysfunction. **A**, EL4mCD19 tumor-bearing C57BL/6 mice, not pretreated with cyclophosphamide, were treated with CAR T cells 1 day after tumor inoculation. Data were obtained from two independent experiments ( $n = 5-9$  mice per group). Significance was determined through log-rank Mantel-Cox test, with 95% confidence interval. \*,  $P = 0.0022$  m19ζIL12 compared with m19BBζIL12; \*,  $P = 0.0042$  m19ζIL12 compared with m1928ζIL12; and "ns" m1928ζIL12 compared with m19BBζIL12. **B**, CAR T cells were isolated by FACS from the bone marrow, selected for CD8<sup>+</sup> T cells, cocultured with EL4mCD19 tumor targets, and then assessed for cytotoxicity 24 hours later, using a luciferase killing assay. Data shown are mean ± SEM of two independent experiments ( $n = 4-6$  mice per group). Significance determined by one-way ANOVA: \*,  $P = 0.0155$  m19ζIL12 compared with m1928ζIL12; \*,  $P = 0.0394$  m19ζIL12 compared with m19BBζIL12; and ns m1928ζIL12 compared with m19BBζIL12. ns, not significant.

investigation of the mechanisms of how CAR T-cell dysfunction is induced in patients treated with CD19 targeted CAR T cells is necessary to determine if costimulation driven dysfunction is a factor in CAR T-cell treatment failure.

More costimulation is thought to enhance antitumor efficacy. Herein, we demonstrate that too much or too little costimulation can both be deleterious to *in vivo* CAR T-cell antitumor function. Within this "goldilocks" principle of T-cell costimulation, our data support further investigation into optimizing CAR T-cell *in vivo* costimulation. Here, we provide evidence demonstrating that excessive costimulation drives T-cell dysfunction in adoptively transferred tumor-targeting T cells. CAR T cells need a balance of T-cell activation signals for effective antitumor function. CAR T cells must be designed to reflect this balance. Previous reports have suggested that too much CD3ζ signaling can render a CAR T cell dysfunctional and have suggested that the dampening of CAR CD3ζ signaling can improve CAR T-cell efficacy (25). Our results extend these findings by demonstrating that too much costimulation will also lead to CAR T-cell dysfunction. This report describes a mechanism of inducing CAR T-cell dysfunction that can be exploited in the design of future CAR T-cell therapies to prevent CAR T-cell dysfunction and improve the efficacy of CAR therapies.

### Disclosure of Potential Conflicts of Interest

R.J. Brentjens reports receiving grant support from JUNO Therapeutics (a Bristol-Myers Squibb company) and is a consultant/advisor for Gracell Biotechnologies, Inc. No potential conflicts of interest were disclosed by the other authors.

### Authors' Contributions

**Conception and design:** D. Wijewarnasuriya, C. Bebernitz, S. Rafiq, R.J. Brentjens  
**Development of methodology:** D. Wijewarnasuriya, C. Bebernitz, S. Rafiq, R.J. Brentjens

**Acquisition of data (provided animals, acquired and managed patients, provided facilities, etc.):** D. Wijewarnasuriya, C. Bebernitz, R.J. Brentjens

**Analysis and interpretation of data (e.g., statistical analysis, biostatistics, computational analysis):** D. Wijewarnasuriya, C. Bebernitz, S. Rafiq, R.J. Brentjens  
**Writing, review, and/or revision of the manuscript:** D. Wijewarnasuriya, S. Rafiq, R.J. Brentjens

**Administrative, technical, or material support (i.e., reporting or organizing data, constructing databases):** D. Wijewarnasuriya, C. Bebernitz, A.V. Lopez, R.J. Brentjens

**Study supervision:** R.J. Brentjens

### Acknowledgments

The authors acknowledge B. Qeriqi for technical assistance with *in vivo* experiments and J.E. Jaspers, C. Hackett, and E. Smith for critical reading of the article. The authors thank the following for financial support: U.S. National Institutes of Health grants 5 P01 CA190174-03 and 5 P50 CA192937-02 (R.J. Brentjens), The Annual

Terry Fox Run for Cancer Research organized by the Canada Club of New York (R.J. Brentjens), Kate's Team (R.J. Brentjens), Carson Family Charitable Trust (R.J. Brentjens), William H. Goodwin and Alice Goodwin and the Commonwealth Foundation for Cancer Research, and the Experimental Therapeutics Center of Memorial Sloan Kettering Cancer Center (innovations in the structures, functions, and targets of monoclonal antibody-based drugs for cancer; R.J. Brentjens).

The costs of publication of this article were defrayed in part by the payment of page charges. This article must therefore be hereby marked *advertisement* in accordance with 18 U.S.C. Section 1734 solely to indicate this fact.

Received November 15, 2019; revised January 12, 2020; accepted March 19, 2020; published first March 25, 2020.

References

1. Schietinger A, Philip M, Krisnawan VE, Chiu EY, Delrow JJ, Basom RS, et al. Tumor-specific T cell dysfunction is a dynamic antigen-driven differentiation program initiated early during tumorigenesis. *Immunity* 2016;45:389–401.
2. Bucks CM, Norton JA, Boesteanu AC, Mueller YM, Katsikis PD. Chronic antigen stimulation alone is sufficient to drive CD8+ T cell exhaustion. *J Immunol* 2009;182:6697–708.
3. Angelosanto JM, Blackburn SD, Crawford A, Wherry EJ. Progressive loss of memory T cell potential and commitment to exhaustion during chronic viral infection. *J Virol* 2012;86:8161–70.
4. Brooks DG, McGavern DB, Oldstone MBA. Reprogramming of antiviral T cells prevents inactivation and restores T cell activity during persistent viral infection. *J Clin Invest* 2006;116:1675–85.
5. Crawford A, Angelosanto JM, Kao C, Doering TA, Odorizzi PM, Barnett BE, et al. Molecular and transcriptional basis of CD4+ T cell dysfunction during chronic infection. *Immunity* 2014;40:289–302.
6. Wherry EJ, Ha S-J, Kaech SM, Haining WN, Sarkar S, Kalia V, et al. Molecular signature of CD8+ T cell exhaustion during chronic viral infection. *Immunity* 2007;27:670–84.
7. Jin H-T, Anderson AC, Tan WG, West EE, Ha S-J, Araki K, et al. Cooperation of Tim-3 and PD-1 in CD8 T-cell exhaustion during chronic viral infection. *Proc Natl Acad Sci U S A* 2010;107:14733–8.
8. Matsuzaki J, Gnjatic S, Mhawech-Fauceglia P, Beck A, Miller A, Tsuji T, et al. Tumor-infiltrating NY-ESO-1-specific CD8+ T cells are negatively regulated by LAG-3 and PD-1 in human ovarian cancer. *Proc Natl Acad Sci U S A* 2010;107:7875–80.
9. Thommen DS, Schumacher TN. T cell dysfunction in cancer. *Cancer Cell* 2018;33:547–62.
10. Wherry EJ. T cell exhaustion. *Nat Immunol* 2011;12:492–9.
11. Pauken KE, Wherry EJ. Overcoming T cell exhaustion in infection and cancer. *Trends Immunol* 2015;36:265–76.
12. Brentjens RJ, Santos E, Nikhamin Y, Yeh R, Matsushita M, La Perle K, et al. Genetically targeted T cells eradicate systemic acute lymphoblastic leukemia xenografts. *Clin Cancer Res* 2007;13:5426–35.
13. Brentjens RJ, Latouche J-B, Santos E, Marti F, Gong MC, Lyddane C, et al. Eradication of systemic B-cell tumors by genetically targeted human T lymphocytes co-stimulated by CD80 and interleukin-15. *Nat Med* 2003;9:279–86.
14. Wang X, Rivière I. Clinical manufacturing of CAR T cells: foundation of a promising therapy. *Mol Ther Oncolytics* 2016;3:16015.
15. Rafiq S, Hackett CS, Brentjens RJ. Engineering strategies to overcome the current roadblocks in CAR T cell therapy. *Nat Rev Clin Oncol* 2020;7:147–67.
16. Maher J, Brentjens RJ, Gunset G, Rivière I, Sadelain M. Human T-lymphocyte cytotoxicity and proliferation directed by a single chimeric TCR $\zeta$ /CD28 receptor. *Nat Biotechnol* 2002;20:70–5.
17. Brentjens RJ, Riviere I, Park JH, Davila ML, Wang X, Stefanski J, et al. Safety and persistence of adoptively transferred autologous CD19-targeted T cells in patients with relapsed or chemotherapy refractory B-cell leukemias. *Blood* 2011;118:4817–28.
18. Park JH, Rivière I, Gonen M, Wang X, Sénéchal B, Curran KJ, et al. Long-term follow-up of CD19 CAR therapy in acute lymphoblastic leukemia. *N Engl J Med* 2018;378:449–59.
19. Davila ML, Riviere I, Wang X, Bartido S, Park J, Curran K, et al. Efficacy and toxicity management of 19-28z CAR T cell therapy in B cell acute lymphoblastic leukemia [Internet]. *Sci Transl Med* 2014;6:224ra25
20. Maude SL, Frey N, Shaw PA, Aplenc R, Barrett DM, Bunin NJ, et al. Chimeric antigen receptor T cells for sustained remissions in leukemia. *N Engl J Med* 2014;371:1507–17.
21. Porter DL, Hwang WT, Frey N V., Lacey SF, Shaw PA, Loren AW, et al. Chimeric antigen receptor T cells persist and induce sustained remissions in relapsed refractory chronic lymphocytic leukemia. *Sci Transl Med* 2015;7:1–13.
22. Turtle CJ, Hanafi LA, Berger C, Gooley TA, Cherian S, Hudecek M, et al. CD19 CAR-T cells of defined CD4+: CD8+ composition in adult B cell ALL patients. *J Clin Invest* 2016;126:2123–38.
23. Geyer MB, Rivière I, Sénéchal B, Wang X, Wang Y, Purdon TJ, et al. Autologous CD19-targeted CAR T cells in patients with residual CLL following initial purine analog-based therapy. *Mol Ther* 2018;26:1896–905.
24. Long AH, Haso WM, Shern JF, Wanhainen KM, Murgai M, Ingaramo M, et al. 4-1BB costimulation ameliorates T cell exhaustion induced by tonic signaling of chimeric antigen receptors. *Nat Med* 2015;21:581–90.
25. Feucht J, Sun J, Eyquem J, Ho YJ, Zhao Z, Leibold J, et al. Calibration of CAR activation potential directs alternative T cell fates and therapeutic potency. *Nat Med* 2019;25:82–8.
26. Moon EK, Wang LC, Dolfi DV, Wilson CB, Ranganathan R, Sun J, et al. Multifactorial T-cell hypofunction that is reversible can limit the efficacy of chimeric antigen receptor-transduced human T cells in solid tumors. *Clin Cancer Res* 2014;20:4262–73.
27. Galon J, Rossi J, Turcan S, Danan C, Locke FL, Neelapu S, et al. Characterization of anti-CD19 chimeric antigen receptor (CAR) T cell-mediated tumor micro-environment immune gene profile in a multicenter trial (ZUMA-1) with axicabtagene ciloleucel (axi-cel, KTE-C19). *J Clin Invest* 2017;35:3025.
28. Zolov SN, Rietberg SP, Bonifant CL. Programmed cell death protein 1 activation preferentially inhibits CD28.CAR-T cells. *Cytotherapy* 2018;20:1259–66.
29. Pegram HJ, Lee JC, Hayman EG, Imperato GH, Tedder TF, Sadelain M, et al. Tumor-targeted T cells modified to secrete IL-12 eradicate systemic tumors without need for prior conditioning. *Blood* 2012;119:4133–41.
30. Davila ML, Kloss CC, Gunset G, Sadelain M. CD19 CAR-targeted T cells induce long-term remission and B cell aplasia in an immunocompetent mouse model of B cell acute lymphoblastic leukemia. *PLoS One* 2013;8:1–14.
31. Kochenderfer JN, Yu Z, Frasheri D, Restifo NP, Rosenbergs SA. Adoptive transfer of syngeneic T cells transduced with a chimeric antigen receptor that recognizes murine CD19 can eradicate lymphoma and normal B cells. *Blood* 2010;116:3875–86.
32. Lee J, Sadelain M, Brentjens R. Retroviral transduction of murine primary T lymphocytes. *Methods Mol Biol* 2009;506:83–96.
33. Ferrone CR, Perales MA, Goldberg SM, Somberg CJ, Hirschhorn-Cymerman D, Gregor PD, et al. Adjuvanticity of plasmid DNA encoding cytokines fused to immunoglobulin Fc domains. *Clin Cancer Res* 2006;12:5511–9.
34. Smith EL, Staehr M, Masakayan R, Tataka JJ, Purdon TJ, Wang X, et al. Development and evaluation of an optimal human single-chain variable fragment-derived BCMA-targeted CAR T cell vector. *Mol Ther* 2018;26:1447–56.
35. Curtsinger JM, Schmidt CS, Mondino A, Lins DC, Kedl RM, Jenkins MK, et al. Inflammatory cytokines provide a third signal for activation of naive CD4+ and CD8+ T cells. *J Immunol* 1999;162:3256–62.
36. Curtsinger JM, Lins DC, Mescher MF. Signal 3 Determines tolerance versus full activation of Naive CD8 T cells: dissociating proliferation and development of effector function. *J Exp Med* 2003;197:1141–51.
37. Valenzuela J, Schmidt C, Mescher M. The roles of IL-12 in providing a third signal for clonal expansion of naive CD8 T cells. *J Immunol* 2002;169:6842–9.
38. Crespo J, Sun H, Welling TH, Tian Z, Zou W. T cell anergy, exhaustion, senescence, and stemness in the tumor microenvironment. *Curr Opin Immunol* 2013;25:214–21.
39. Vallè A, Aubry J plerre, Durand I, Banchereau J. IL-4 and IL-2 upregulate the expression of antigen B7, the B cell counterstructure to T cell CD28: an amplification mechanism for T-B cell interactions. *Int Immunol* 1991;3:229–36.
40. Yeku OO, Purdon TJ, Koneru M, Spriggs D, Brentjens RJ. Armored CAR T cells enhance antitumor efficacy and overcome the tumor microenvironment. *Sci Rep* 2017;7:1–14.
41. Koneru M, Purdon TJ, Spriggs D, Koneru S, Brentjens RJ. IL-12 secreting tumor-targeted chimeric antigen receptor T cells eradicate ovarian tumors in vivo. *Oncoimmunology* 2015;4:e994446.

Downloaded from <http://aacrjournals.org/cancerimmunolres/article-pdf/8/6/732/25356839/732.pdf> by guest on 22 July 2024

42. Pratiksha J, Rühl M, Pircher Schubert M, Simon M, Haefner S, et al. Aberrant Lck signal via CD28 co-stimulation augments antigen-specific functionality and tumor control by redirected T cells with PD-1 blockade in humanized mice. *Clin Cancer Res* 2018;24:3981–93.
43. Boucher JC, Li G, Shrestha B, Zhang Y, Vishwasrao P, Cabral ML, et al. Mutation of the CD28 costimulatory domain confers increased CAR T cell persistence and decreased exhaustion. *J Immunol* 2018;200 Suppl 1: 57.28.
44. Salter AI, Ivey RG, Kennedy JJ, Voillet V, Rajan A, Alderman EJ, et al. Phosphoproteomic analysis of chimeric antigen receptor signaling reveals kinetic and quantitative differences that affect cell function. *Sci Signal* 2018; 11. pii: eaat6753.
45. Oren R, Hod-Marco M, Haus-Cohen M, Thomas S, Blat D, Duvshani N, et al. Functional comparison of engineered T cells carrying a native TCR versus TCR-like antibody-based chimeric antigen receptors indicates affinity/avidity thresholds. *J Immunol* 2014;193:5733–43.
46. Avanzi MP, Yeku O, Li X, Wijewarnasuriya DP, van Leeuwen DG, Cheung K, et al. Engineered tumor-targeted T cells mediate enhanced anti-tumor efficacy both directly and through activation of the endogenous immune system. *Cell Rep* 2018;23:2130–41.